Two-Dimensional Multichannel Spectroscopy of a Pulsed Arc†

Yoshiaki ARATA*, Shoji MIYAKE** Hidesato MATSUOKA*** and Hiroaki KISHIMOTO***

Abstract

Several calibrations are performed on the application of a two-dimensional optical multichannel analyzer system for spectroscopic study of a pulsed high current arc. It is found we suffer from various problems when we want to use the detector at a very small gating time interval τ_g. For $\tau_g \lesssim 1$ μS, for instance, both the sensitivity and the spectral resolving power become worsened nonlinearly with τ_g over the surface, especially near the edge of the target. Various data processing techniques are inherently necessary to have a correct measurement of the emitted spectra. In spite of these problems a very efficient and reliable detection is insisted on by some experimental results of the pulsed arc.

KEY WORDS: (Multichannel Spectroscopy) (Pulsed Arc) (Two-Dimensional Detector)

1. Introduction

In the previous paper[1] we reported on the spectroscopic study of a pulsed high current arc by using an optical multichannel analyzer (OMA, PAR). There one-dimensional in-situ spectra were investigated and a strong influence of the gating pulse waveform on the line profile measurement was demonstrated for the time resolved spectroscopy. This influence by no means came mainly from the electron optical nature of the image intensifier in the SIT detector.

We recently equipped a two-dimensional analyzer system (OMA2, PAR) to have a more efficient and relible information of a pulsed radiation phenomenon. This system is still applicable mainly for visible region of the wavelength with a high quantum efficiency. As we have already suffered from many problems on the correct usage of the one-dimensional detector, it is quite reasonable to calibrate all the problems we can consider for this system, even if PAR specifies a good and reliable characters of the detector. For instance, how will sensitivity and resolving power of the detector will change with the gating pulse width ? Surprisingly strong nonlinear variation, especially on the sensitivity, occurs on the detector target as we can see below.

In this paper we report several calibaration procedures of this analyzer system, comparing sometimes with a one= dimensional one. Also some characteristic behaviors of the pulsed arc studied by using this analyzer system are described mainly in the early stage of the time development.

2. Experimental apparatus and methods

The experimental apparatus we use is the same as the one described in ref. 1). As for the two-dimensional multichannel analyzer (OMA2), the dimension (12.5 x 12.5 mm) of the detector's sensitive area and the vidicon scanning pattern are shown schematically in **Fig. 1**. When the detector is mounted on the exit of a monochromator,

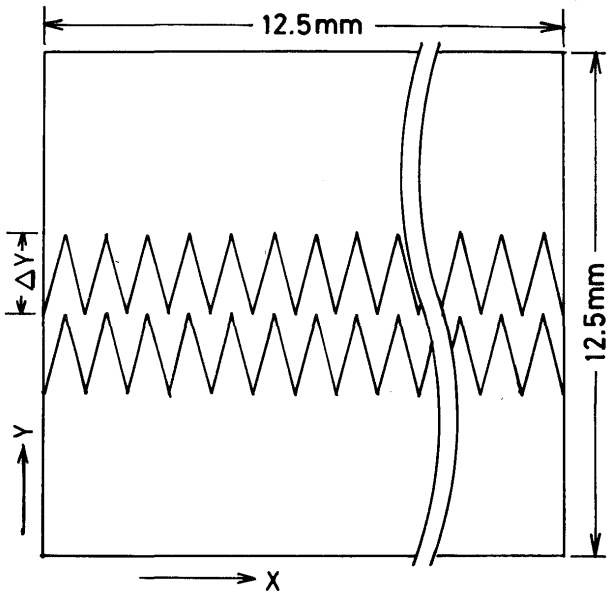

Fig. 1 Dimension and vidicon scanning patterns on the sensitive area of a two-dimensional silicon intensified target detector.

† Received on March 31, 1981
* Professor
** Associate Professor
*** Graduate Student

Transactions of JWRI is published by Welding Research Institute of Osaka University, Suita, Osaka, Japan

the horizontal 500 channels in x-direction usually correspond to the wavelength and the vertical ones in y-direction to the height of the entrance slit image. So that by dividing y-direction with many segments of Δy, which is called "track", we can obtain a spatial intensity distribution of emitted spectra along the entrance slit of the monochromotor. Each channel has 25μm in length and the minimum of a track is specified to be 4 channels. When the entrace slit is parallel to the radial direction of the arc column, a lateral intensity distribution of a line profile is thus obtained at each shot of the experiment.

3. Calibration of two-dimensional detector

3.1 Shift of a spectral line on the target surface

Since the detector target has wide rectangular surface, the line shift is more clearly seen than in the one-dimensional detector described in the previous paper.

By using a 25 cm monochromator (1st-order inverse dispersion 32A/mm) and a Cd lamp, we measured the position where the peak intensity of CdI 4800A line occurs, by fixing the central wavelength of the monochromator at various values. In this case x-direction of the target covers 400A by 500 channels and Δy is selected to be 16 channels with the gating voltage V_g = –1.25kV, the gating pulse width τ_g = 100μS. **Figure 2** shows a mapping of these positions for 9 selected values of the wavelength. Around the corner of the target, clear distortion is observed by 10–20 channels in x-direction. This problems is serious when we want to know the velocity of particles by the Doppler shift of a spectral line.

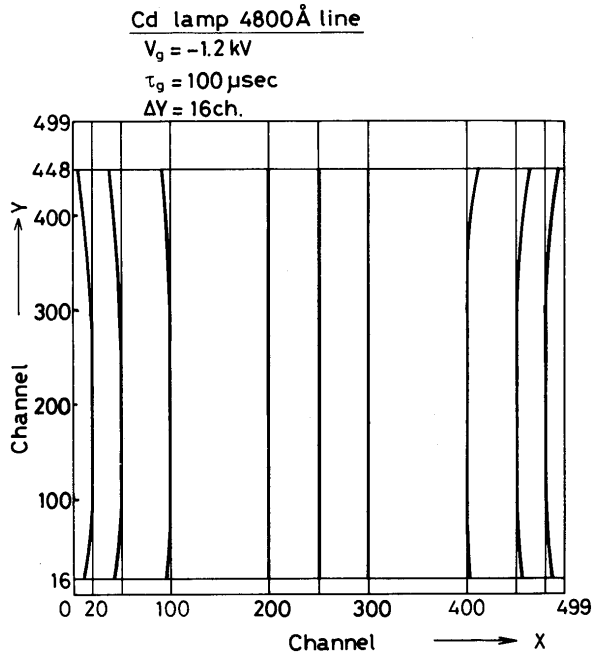

Fig. 2 Typical image distortion on the target tested by using CdI 4800A line.

3.2 Sensitivity and resolving power of the target

To check these qualities we used at need Cd lamp,

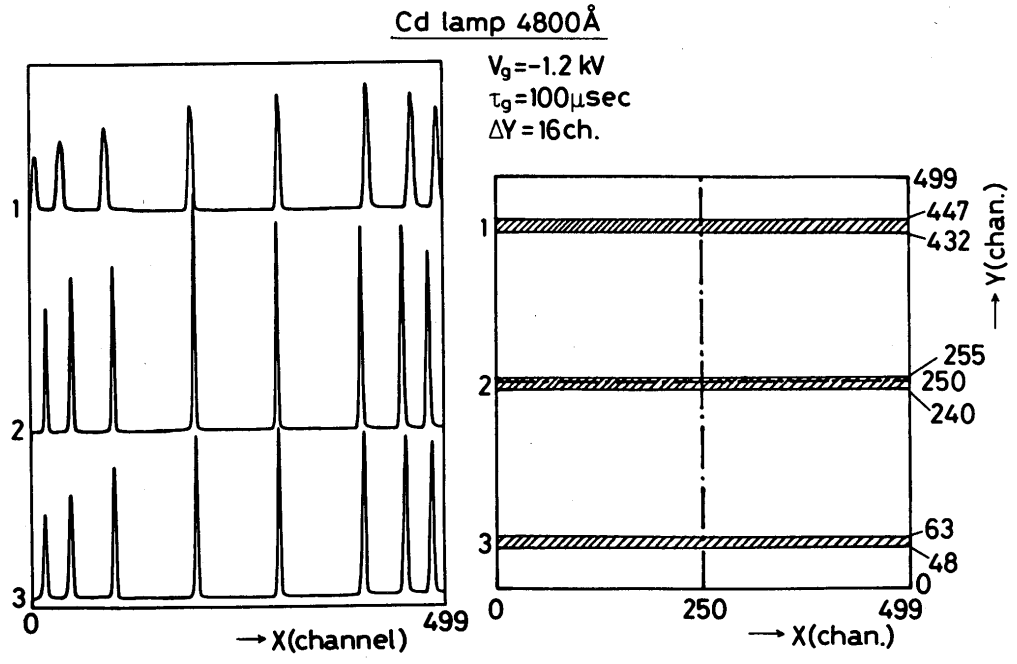

Fig. 3 Spectral response of the detector.
a) CdI 4800A line profiles obtained by fixing the central wavelength of a 25 cm monochromator at various values.
b) Track areas used to measure the CdI 4800A line in the left fugure.

He-Ne laser, W-ribbon lamp in conjunction with the same 25 cm monochromator.

Figure 3 shows an example of the line profiles measured with Cd lamp at the same condition with Fig. 2. On the left it is seen that the halfwidth of CdI 4800A line is larger on the upper and the lower parts of the target, especially on the corner. Also the sensitivity on the periphery decreases to about 1/2 of the center. These features are more clearly seen in **Fig. 4.** On the left of Fig. 4, the peak intensity distribution is mapped in arbitrary units for CdI 4800A line. While on the right, the halfwidth $\Delta\lambda_{1/2}$ of the line is mapped in numbers of channels. Both figures exhibit nearly cocentric circles, since the image intensifier has inherently a cocentric character. So that the efficient usage of the whole rectangular surface is quite difficult, without sufficient cor-

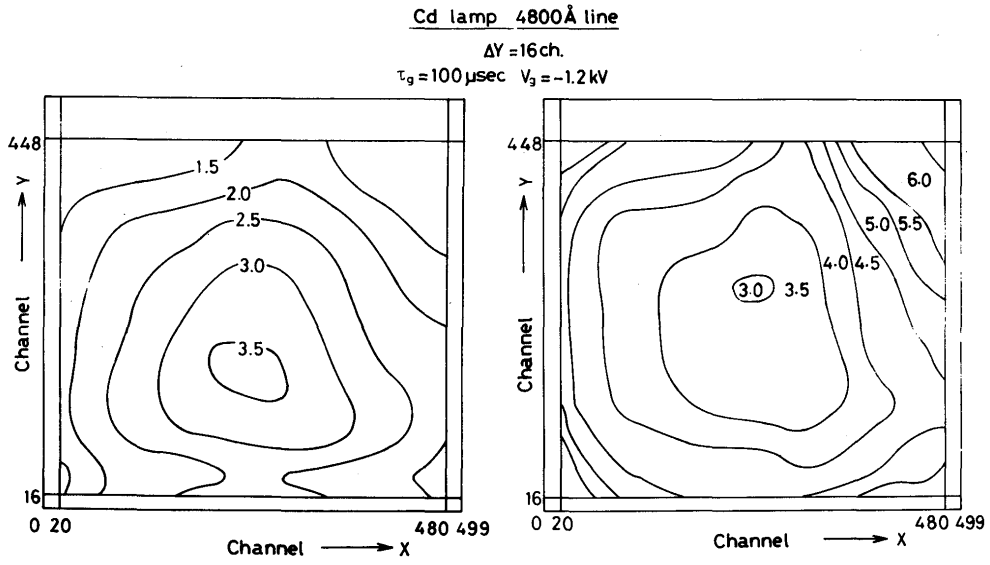

Fig. 4 Mapping of sensitivity and spectral resolving power of the target obtained for CdI 4800A line in case of $V_g = -1.2$-kV, $\tau_g = 100\ \mu$S.

rections or compensations around the corner.

3.3 Changes in resolving power and sensitivity for different gating widths

In Figs. 2-4, the gating pulse width τ_g is selected to be 100 μS. How will the resolving power change when τ_g is varied? **Figure 5** shows a result obtained by using He-Ne laser 6328A line. Since the intensity of CdI 4800A line was not so strong to be able to detect at a very short pulse width, He-Ne laser light was imaged on the 25 cm monochromator. As is clearly seen in the figure, the halfwidth $\Delta\lambda_{1/2}$ measured at the center of the target has a minimum value at $|V_g| = 1.2 - 1.3$ kV. This feature is well known as "voltage focusing"[2]. While when τ_g is smaller than 2.0 μS, $\Delta\lambda_{1/2}$ can no longer be 3-4 channels as is specified by PAR. It increases to 7-8 channels for τ_g= 1.0 or 0.5 μS at the optimum gating voltage. Here we select, of course, a good rectangular waveform to avoid the defocusing effect mentioned in the previous paper. The applied pulse shapes are shown in **Fig. 6.** Moreover we here notice that at $\tau_g = 1.0\ \mu$S, for instance, $\Delta\lambda_{1/2}$

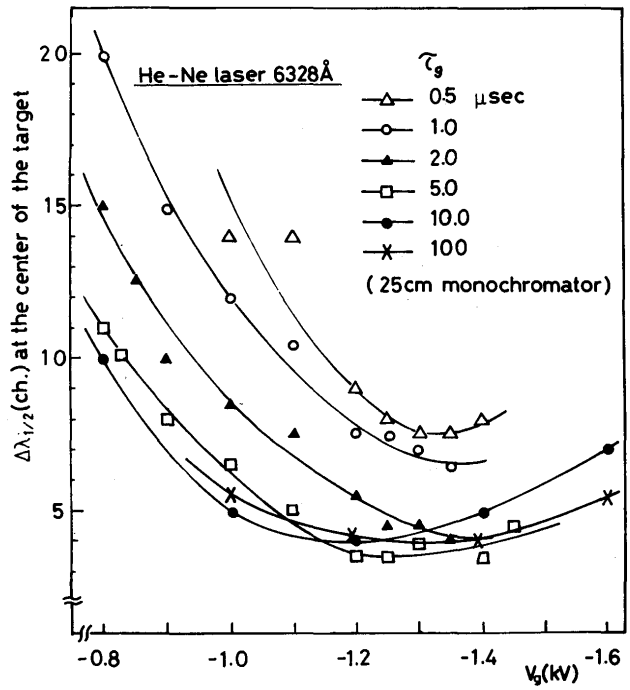

Fig. 5 Variations of the halfwidth $\Delta\lambda_{1/2}$ of CdI 4800A line at the center of the target for different V_g and τ_g.

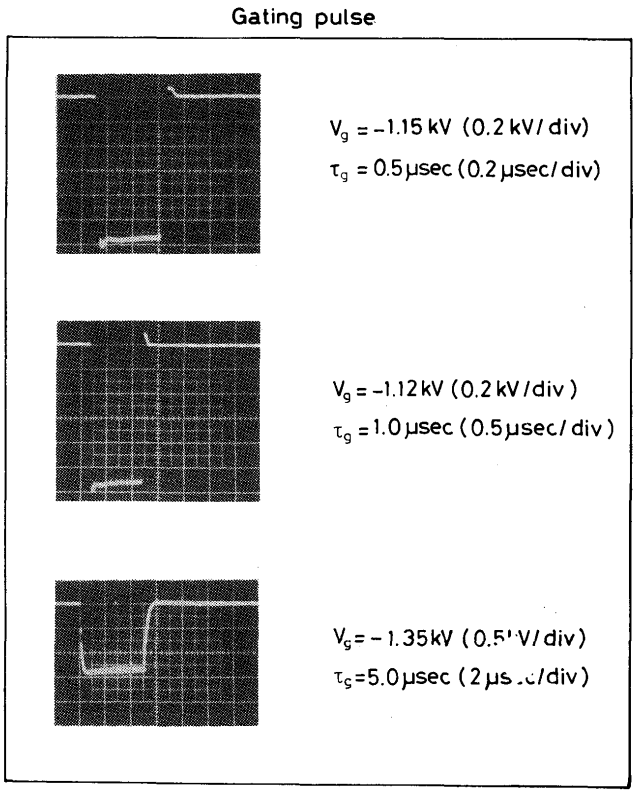

Fig. 6 Gating pulse shapes for different τ_g.

keeps almost a constant value (7-8 channels) on most region of the target, in contrast to the case of τ_g = 100 μS (Fig. 4-b).

Also change of the sensitivity for different τ_g along channels were measured by using a standard W-ribbon lamp (Type-EP, EPLEY). The lamp is imaged on the entrance slit to have a sufficiently uniform intensity distribution along the slit. **Figure 7** shows intensity distributions between 4486 and 4886 A for 3 gating pulses. Among 16 tracks, only the one track's data near the middle part of the target is shown and the intensity is normalized at 4686A for all data. In case of τ_g = 20μS the distribution is almost the same as that of the real time operation. But when τ_g is smaller, the normalized intensity drops in the ranges 0-100 and 400-500 channels, especially at τ_g = 1.0 μS.

From these results we can conclude that we should always have a calibration on the whole surface of the detector, even when we change only one operating parameter of the detector. The operating parameters we may change are gating voltage V_g, gating pulse width τ_g, track dimension Δy, vidicon scanning time or numbers and so on. Needless to say, we must give the same procedure when we change a monochromator. Different patterns in sensitivity and resolving power will naturally be expected even at the same values of V_g, τ_g and Δy.

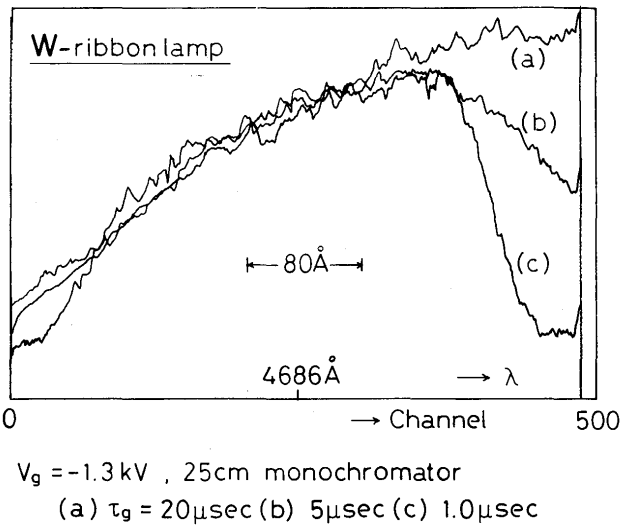

Fig. 7 Spectral response of the light emission from the standard W-ribbon lamp over 400A centered at 4686A. For 3 gating pulse widths all responses are normalized at 4686A.

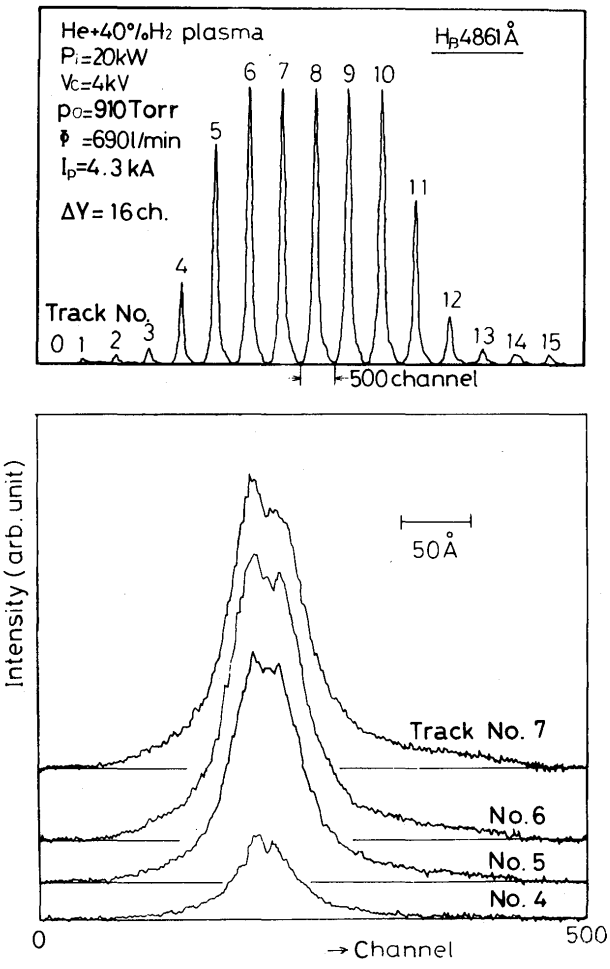

Fig. 8 Typical lateral distribution of Hβ 4861A line profile from the arc at p_o = 910 torr. Δy is selected to be 16 channels.

Furthermore we need rather complicated numerical calculations to correct or compensate variations in sensitivity and resolving power, when we want to use efficiently all the surface of the target. To obtain the same resolving power and the same normalized sensitivity distributions, over the surface as the real time operation mode at a very small gating width, it is good[3,4] to have a light pulse with a shorter pulse width than τ_g, by applying a Kerr shutter or another type of a shutter in front of a monochromator.

So far we described on the calibration procedures by letting Δy = 16 channels. As stated earlier, the minimum Δy is specified to be 4 channels owing to the scanning characteristics of the vidicon in the detector. The resolving power in x-direction showed 7-8 channels in case τ_g = 1.0 μS (See Fig. 5). So that the spatial resolving power in y-direction is expected to be a similar one. To certify it, we rotated the detector in 90 degrees and measured the minimum Δy below which CdI 4800A line smeared out to the neighboring tracks. It gives 8 channels at best, by which we consider the allowable minimum track dimension is 8 channels in y-direction.

4. Time development of a pulsed high current arc

In ref. 1) we described some characteristics of a pulsed arc studied by a one-dimensional detector. Here we can obtain much more efficiently many informations with a two-dimensional one at each shot. By irradiating nearly the half area of the detector, we measured lateral distributions of various spectra. The track width Δy was selected to be 8 or 16 channels and τ_g was fixed to be 1.0 μS with V_g = −1.3 kV. It is shown on the upper part of **Fig. 8** an example of the lateral distribution of H_β 4861A line profiles in case of Δy = 16ch.. The lower part gives the line profiles enlarged in wavelength at several tracks. In **Fig. 9** is shown a similar distribution in case of Δy = 8ch. for other external parameters of the arc. On the left He II 4686A lines are detected only in the central region of the arc where H_β 4861A line radiates more weakly than on the periphery. These data are obtained shot by shot with quite a good S/N ratio. Indeed they are raw data and various corrections should be performed by using a computor as stated in the previous section.

Figure 10 shows the time development of electron density n_e averaged over radius for two cases of the external parameters of the arc. In case of He + 40% H_2 plasma n_e reaches to the first maximum of about 1.8×10^{17} cm^{-3} at $t \simeq 6$ μS. While for He + 80% H_2 plasma it occurs at a very short time of $t \simeq 1$ μS. This difference comes from that of the current density in the initial stage of the Joule heating, since the initial plasma radius is 2

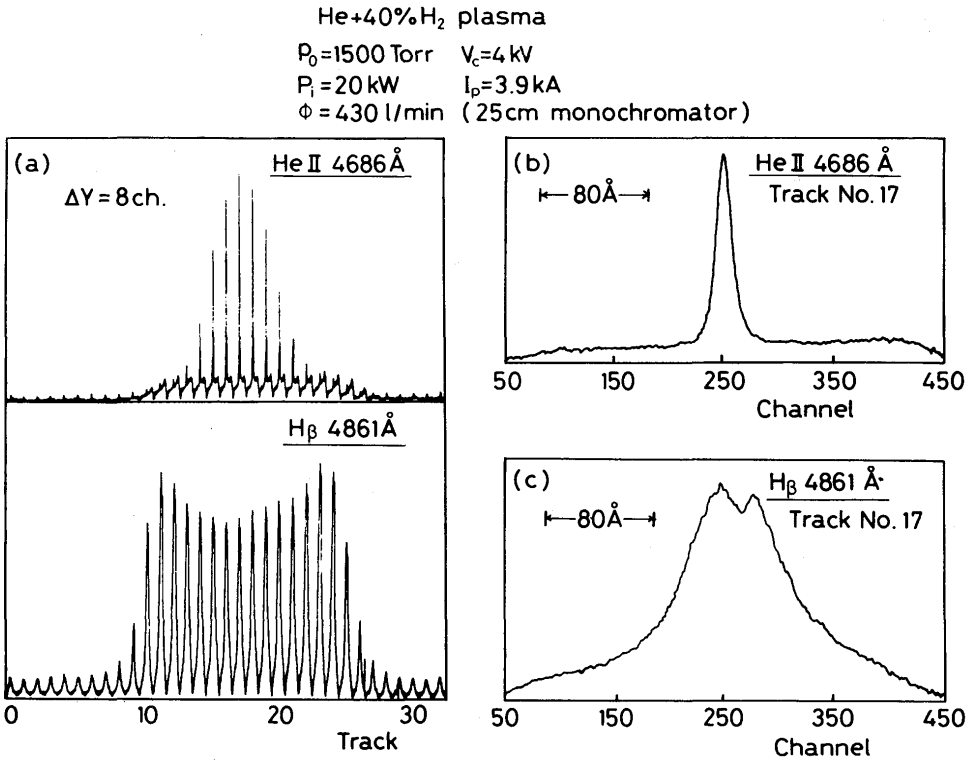

Fig. 9 Typical lateral distribution of HeII 4686A and $H\beta$ 4861A line profiles from the arc at p_o = 1520 torr. Δy is selected to be 8 channels.

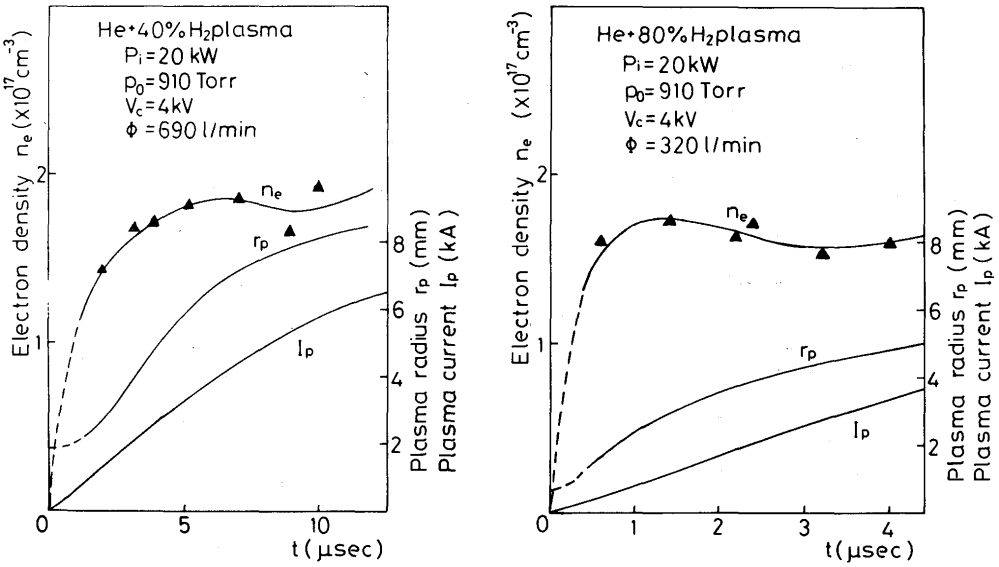

Fig. 10 Time development of electron density n_e, plasma radius r_p and plasma current I_p for two experimental conditions of the arc.

mm in the former and 1 mm in the latter with a little larger rate of the current increase. In the figure n_e is decided from Stark broadening of H_β line profile and r_p from the lateral distribution of H_β line total intensity. We are now under study of the complex temporal behaviors of the arc for various experimental conditions applying data processing techniques, and the detailed results will be reported elsewhere.

5. Conclusion

Several problems were studied on the application of a two-dimensional optical multichannel analyzer system (OMA2, PAR) for a spectroscopic study of a pulsed arc. As the analyzer is mounted with a cylindrical image intensifier in front of the silicon target, it is possible to have a gate mode operation with a good time resolution of light emission. However, in turn it causes serious problems, especially in two-dimensional data acquisition, on the correct transformation of photon signals on to the target by photoelectrons, owing to various electron optical problems of the intersifier:

1) Typical two-dimensional patterns of sensitivity and resolving power of the detector have cocentric characters in amplitudes. So that it is very difficult to use efficiently the whole rectangular surface of the target.
2) When the gating pulse width is decreased below several microseconds, the applicable area of the target decrease to a value below 1/2 of the specified 12.5 x 12.5 mm, due to the nonlinear lowering of sensitivity around the edge of the target.
3) Various data processing techniques must be applied to have good compensations to the variable nonuniformities in sensitivity and resolving power. These nonuniformities always appear when we change even one operating parameter of the detector.

Nevertheless, we can successfully obtain many informations we need from the one shot of the discharge of a pulsed arc. This enables us to study in detail the complex temporal behaviors of the arc for different external parameters, with very high efficiency and reliability after appropriate data processing with a computor.

References

1) Y. Arata, S. Miyake, Y. Yoshioka and H. Matsuoka: Trans. of JWRI 9 (1980) 47.
2) W. T. Chiang and Hans R. Griem: Phys. Rev. A18 (1978) 1169.
3) R. W. Simpson and Y. Talmi: Rev. Sci. Instrum. 48 (1977) 1295.
4) G. F. Albrecht, E. Kalne and J. meyer: Rev. Sci, Instrum. 49 (1978) 1637.